A new rod model for the folding and deployment of tape springs with highly deformable cross-sections

Elia Picault, Stéphane Bourgeois, Bruno Cochelin, François Guinot, Christian Hochard

IASS-IACM 2012
GF Sarajevo, Bosnia and Herzegovina
Ibrahimbegovic, Dolarevic, Hrasnica
Madzarevic, Zlatar (eds.)

A new rod model for the folding and deployment of tape springs with highly deformable cross-sections.

E. Picault[1], S. Bourgeois[1,2], B. Cochelin[1,2], F. Guinot[3], C. Hochard[1]

[1] *LMA, Laboratoire de Mécanique et d'Acoustique, Marseille, France, {picault,hochard}@lma.cnrs-mrs.fr*
[2] *Ecole Centrale Marseille, France, {stephane.bourgeois,bruno.cochelin}@centrale-marseille.fr*
[3] *Thales Alenia Space, Cannes La Bocca, France, {francois.guinot}@thalesaleniaspace.com*

Abstract — This work is focused on the modeling of rod-like elastic bodies with thin-walled curved cross-sections such as tape springs, which develop localized folds due to a flattening of the cross-section. Starting from a complete nonlinear elastic shell model, a rod model with highly deformable cross-section is derived for large displacements, large rotations and dynamics, by introducing an elastica kinematics to describe the in-plane changes of the cross-section shape. This model is able to handle the formation of localized folds which can move along the rod line, merge or split, allowing simulation of complex scenarios of coiling, folding and deployment.

Key-words — rod, tape spring, fold, dynamics.

1 Introduction

A major challenge for satellites manufacturers is to develop ingenious compact (for transport and storage) systems capable of deploying themselves in an autonomous way during the set up. Since they offer better compacity (folding, coiling), deployable elastic structures are an interesting alternative to articulated rigid structures with hinges and bolts. In this framework, Thales Alenia Space is working on new concepts based on structures using tape springs. Slender elatic structures, of which tape springs are only an example, have been widely studied in the nonlinear framework because they can suffer from geometrical instabilities that can lead to a sudden loss of stiffness and extreme deformation shapes. The various applications of such structures not only in the aerospace field [9] [10], but also in biophysics, biomechanics or even in micro or nanomechanics [14] are as many motivations to develop robust models of nonlinear elastic structures [1] [12].

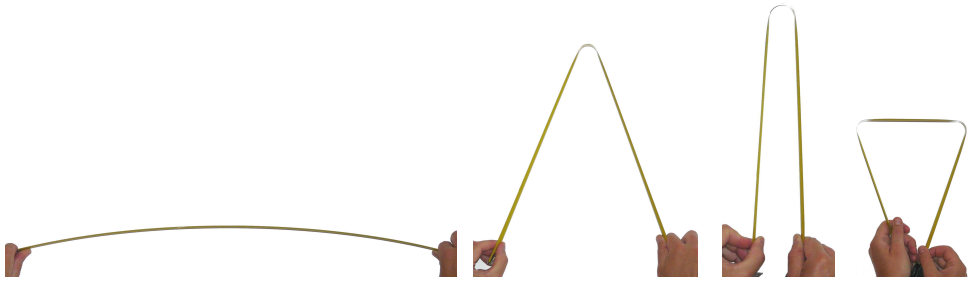

Figure 1: Folding of a tape spring.

In its free state, a tape spring can be assimilated to a straight thin-walled beam with a circular open cross-section of constant transverse curvature. Under progressively applied bending or compressive loads (see Figure 1), this structure behaves at first like a beam before the sudden appearance of localized folds, indicating snap-through buckling [10]. These folds are created thanks to a localized flattening of the cross-sections which drastically reduces the moment of inertia and concentrates the bending deformation in the fold area. We shall note that away from the fold the tape spring remains almost straight and

undeformed. Playing with a carpenter's measure tape, one can easily experience the formation of one or several folds, the motion of a fold along the tape, the splitting of a single fold into two or the merging of two folds into one...

The modeling of tape springs in particular has already been addressed in literature and can be classified into two main approches. The first one consists in the full computation of the nonlinear shell model in the framework of large displacements, large rotations and dynamics [7] [11] [15]. This approach leads to hard to drive calculations and heavy simulations but provides accurate static and dynamic solutions for any loading configurations and boundary conditions. Whereas the first approach does not account for tape spring specificities, the second one is based on the observation that away from the fold the spring remains straight and undeformed. In this approach the tape is therefore modeled using discrete articulated bars [10]: spiral springs, of appropriate moment-rotation characteristic, render the stiffness of the fold areas and rigid bars, of variable length, represent the regions that remain straight. This kind of model makes the simulation of a large panel of deployment scenarios easy but requires the introduction of the folds *ab initio*.

The model proposed herein is intermediate between those two approaches. It is derived from a non-linear shell model which has been reduced to a one dimensional continuous rod-like model including cross-section changes by taking into account the spring specificities (overall rod-like shape, creation of localized folds). Beam models with deformable cross-sections have already been published in literature [13] [8] [3]. The main idea is always to incorporate kinematic parameters to describe in-plane and out-of-plane (wraping) relative displacements. The present work follows theses approaches but takes into account the possibility of large relative displacements in the cross-section with a kinematics more suitable for modeling tape spring behavior. The model obtained, which can manage the creation of new folds, is appropriate for simulating complex folding and deployment scenarios [5] [6].

2 The rod model

2.1 Kinematic description and basic assumptions

A tape spring is regarded as a rod, and is represented by an initially straight rod line and a planar circular cross-section curve, as shown in Figure 2. The fixed orthonormal frame $(O, \mathbf{e_1}, \mathbf{e_2}, \mathbf{e_3})$ is chosen such that the axis $(O, \mathbf{e_1})$ contains the rod line and that the plane $(O, \mathbf{e_1}, \mathbf{e_3})$ is the plane of symmetry of the cross-section curve.

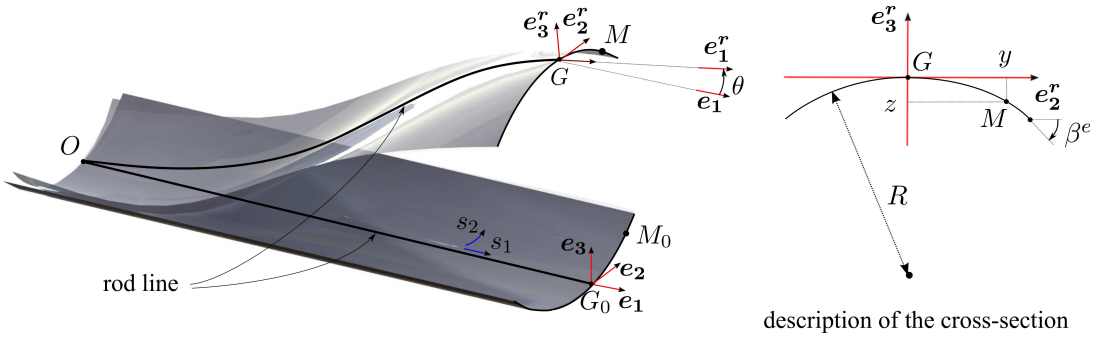

Figure 2: Representation of a tape spring.

We introduce a curvilinear coordinate system $(s_1, s_2) \in [0, L] \times [-a/2, a/2]$ to describe the geometry of the tape, with L the initial length of the rod line and a the initial length of the cross-section curve. In the deformed configuration, the position of a material point M is given by:

$$\mathbf{OM} = \mathbf{OG} + \mathbf{GM}, \tag{1}$$

where G is the point of the cross-section attached to the rod line.

For simplicity, we restricted our study to the plane case: the motion of the rod line is restrained to the plane $(O,\mathbf{e_1},\mathbf{e_3})$ and the cross-section curve, initially symmetric with respect to this plane, is assumed to remain symmetric in any deformed configuration. Thus the cross-section position is given by:

$$\mathbf{OG} = [s_1 + u_1(s_1,t)]\,\mathbf{e_1} + u_3(s_1,t)\,\mathbf{e_3}\,, \tag{2}$$

where $u_1(s_1,t)$ and $u_3(s_1,t)$ are the translations of the material point G.

The proposed rod model kinematics relies on three assumptions:

(i) the cross-section curve remains in a plane after deformation,
(ii) the section plane is orthogonal to the tangent vector of the rod line in the deformed configuration,
(iii) the cross-section curve is considered inextensible.

The two first assumptions are classical hypotheses of Euler-Bernoulli beam theory. Assumption (i) makes it possible to introduce a rotated frame $\left(G,\mathbf{e_1^r},\mathbf{e_2^r},\mathbf{e_3^r}\right)$, image of the frame $(G,\mathbf{e_1},\mathbf{e_2},\mathbf{e_3})$ through the rotation of angle $\theta(s_1,t)$ around the axis $\mathbf{e_2}$ ($\mathbf{e_1^r}$ is a unit vector orthogonal to the section plane in the deformed configuration, $\mathbf{e_2^r}$ is set to $\mathbf{e_2}$ and $\mathbf{e_3^r} = \mathbf{e_1^r} \times \mathbf{e_2^r}$). Whereas assumption (ii) implies that the vector $\mathbf{e_1^r}$ is colinear to the natural rod line tangent vector $\mathbf{a_1^r}$.

The coordinates of the material point M in the local frame $\left(G,\mathbf{e_2^r},\mathbf{e_3^r}\right)$ are given by $y(s_1,s_2,t)$ and $z(s_1,s_2,t)$. Thus assumption (iii), which amounts to introducing an *elastica* to describe the kinematics of the cross-section curve, leads to the following relation:

$$(\mathbf{GM})_{,2} \cdot (\mathbf{GM})_{,2} = (y_{,2})^2 + (z_{,2})^2 = (y_{0,2})^2 + (z_{0,2})^2 = 1\,, \tag{3}$$

where $X_{,i}$ stands for the partial derivative of X with respect to s_i. By introducing the angle $\beta(s_1,s_2,t)$ between the tangent to the cross-section curve and the vector $\mathbf{e_2^r}$ (see Figure 2), we get:

$$y_{,2} = \cos\beta \quad \text{and} \quad z_{,2} = \sin\beta\,. \tag{4}$$

When making assumption (iii), we suppose that the most important effect governing the changes in the cross-section shape is the adjustment of the overall bending inertia of the rod in order to minimize its elastic energy: the flattening of the cross-section concentrates the bending deformation and makes the formation of localized folds possible. In doing so we also suppose that transverse strains can be neglected and that the inextensibility assumption is enough to describe the overall shape of the cross-section curve. It is thus possible to use only one kinematic parameter $\beta(s_1,s_2,t)$ to describe the behavior of the cross-section for large displacements and large rotations. This way to parametrize the cross-section curve is clearly inspired by the *Elastica* theory [2] [4].

Moreover, we suppose that the cross-section curve stays circular. Therefore the curvature radius can be written as a linear function of s_2:

$$\beta(s_1,s_2,t) = \frac{2s_2}{a}\beta^e(s_1,t)\,, \tag{5}$$

where $\beta^e(s_1,t) = \beta\left(s_1, s_2 = \frac{a}{2}, t\right)$.

This expression of β makes it possible to go back from the expressions of $y_{,2}$ and $z_{,2}$ to the local coordinates y and z:

$$\begin{aligned} y(s_1,s_2,t) &= \int_0^{s_2} y_{,2}(s_1,s_2,t)\,d\xi = \int_0^{s_2} \cos\beta(s_1,\xi,t)\,d\xi = \frac{a}{2\beta^e}\sin\left(2\beta^e\frac{s_2}{a}\right), \\ z(s_1,s_2,t) &= \int_0^{s_2} z_{,2}(s_1,s_2,t)\,d\xi = \int_0^{s_2} \sin\beta(s_1,\xi,t)\,d\xi = \frac{a}{2\beta^e}\left(1-\cos\left(2\beta^e\frac{s_2}{a}\right)\right). \end{aligned} \tag{6}$$

Finally the tape spring kinemtatics is totally described by only four kinematic parameters attached to the rod line and functions of s_1, s_2 and t:

(i) the translations u_1 and u_3 of the cross-section,
(ii) the rotation θ of the cross-section around $\mathbf{e_2}$,
(iii) and the angle β characterizing the shape of the cross-section.

The approach presented herein for a cross-section shape and a kinematics relatively simple may be generalized to more complex shapes or kinematics by choosing an appropriate discretization (e.g. Ritz, FE, etc.) of the angle $\beta(s_1,s_2,t)$ with respect to the transverse coordinate s_2 and by adding some kinematic parameters. At this time we are working on generalizing our approach to non-symmetric displacements including out-of-plane bending and torsion.

2.2 Strains measures and strain energy

The tape spring is first regarded as a thin shell. The strain energy is thus calculated using the membrane $e_{\alpha\beta}$ and bending $k_{\alpha\beta}$ strains defined respectively by the Green-Lagrange tensor and by the difference between the initial and actual curvature tensors of the shell. All tensors are expressed thanks to the kinematic parameters u_1, u_3, θ and β.

The strain energy is therefore set to its usual expression for a shell:

$$U_e(u_1,u_3,\theta,\beta) = \int_0^L \int_{-a/2}^{a/2} \frac{1}{2}\left(e_{\alpha\beta}N_{\alpha\beta} + k_{\alpha\beta}M_{\alpha\beta}\right)\, ds_2\, ds_1. \tag{7}$$

where $N_{\alpha\beta}$ and $M_{\alpha\beta}$ are respectively the membrane stresses and bending moments.

Since the shell width a is small compared to the tape spring length L, we suppose that $N_{22} = N_{12} = 0$ according to classical beam theory assumptions. Moreover the shell is considered elastic and orthotropic without any membrane-bending coupling. Thus the constitutive equations of the shell are written:

$$N_{11} = A e_{11} \qquad M_{11} = D_1 k_{11} + D_3 k_{22} \qquad M_{22} = D_3 k_{11} + D_2 k_{22} \qquad M_{12} = D_4\,(2k_{12})$$

with A, D_1, D_2, D_3 and D_4 the elastic constants of the shell.

The shell thickness is also very small compared to the length of the cross-section curve. Thus local and global buckling will prevent large strains to occur, making the assumption of small membrane strains possible. Moreover only the tensile membrane strain e_{11} is needed due to the previous assumptions on N_{12} and N_{22}. The simplified expressions for the membrane strains and bending curvatures are then:

$$\begin{aligned} e_{11} &= e^r + z\,k^r + e^s \\ k_{11} &= -k^r\cos\beta + k^s_{11} \\ k_{22} &= k^s_{22} \\ k_{12} &= k^s_{12} \end{aligned} \tag{8}$$

$$\text{where} \quad \begin{cases} e^r = u_{1,1} + \dfrac{1}{2}\left(u_{1,1}^2 + u_{3,1}^2\right) \\ k^r = \theta_{,1} \end{cases} \quad \text{and} \quad \begin{cases} e^s = \dfrac{1}{2}\left(y_{,1}^2 + z_{,1}^2\right) \\ k^s_{11} = z_{,11}\cos\beta - y_{,11}\sin\beta \\ k^s_{22} = \beta_{,2} - \beta_{0,2} \\ k^s_{12} = \beta_{,1} \end{cases}$$

Expression 8 shows strains (exponent r) induced by the global rod kinematics - usual tensile strain e^r and bending curvature k^r for large displacements and large rotations - and strains (exponent s) induced by the cross-section evolution - e^s and $k^s_{\alpha\beta}$ only depending on the angle β - which constitute the model originality.

Finally, the strain energy can be split into three parts leading to $U_e = U_e^r + U_e^s + U_e^{rs}$, with:

$$\begin{cases} U_e^r = \displaystyle\int_0^L \frac{1}{2}\left(A\,a\,(e^r)^2 + \left(A\,\overline{z^2} + D_1\,\overline{\cos^2(\beta)}\right)(k^r)^2 + 2A\,\bar{z}\,e^r k^r\right) ds_1 \\ U_e^s = \displaystyle\int_0^L \frac{1}{2}\left(A\,\bar{(e^s)}^2 + D_1\,\overline{(k_{11}^s)^2} + D_2\,\overline{(k_{22}^s)^2} + 2D_3\,\overline{k_{11}^s\,k_{22}^s} + 4D_4\,\overline{(k_{12}^s)^2}\right) ds_1 \\ U_e^{rs} = \displaystyle\int_0^L \left(A\,e^r\,\overline{e^s} + A k^r\,\overline{z\,e^s} - k^r\left(D_1\,\overline{\cos(\beta)\,k_{11}^s} + D_3\,\overline{\cos(\beta)\,k_{22}^s}\right)\right) ds_1 \end{cases} \tag{9}$$

where the overline denotes an integration with respect to s_2: $\overline{X}(s_1,t) = \displaystyle\int_{-a/2}^{a/2} X(s_1,s_2,t)\,ds_2$.

In the model presented in Section 2 all these integrals can be calculated analytically, leading to an explicit expression of the strain energy density depending on the kinematic parameters and geometric characterisitcs of the tape spring. The first term U_e^r corresponds to the classical strain energy of a rod with a coupling between axial streching and bending which appears because the rod line does not pass through the cross-section centroid. The second term U_e^s only depends on the variable β and represents the strain energy due to the variation of the cross-section shape, independently of the overall rod behavior. The last term U_e^{rs} introduces a coupling between the overall rod behavior and the variation of the cross-section shape.

2.3 Kinetic energy

Starting from the kinetic energy of the initial shell model in which the rotation inertia is neglected and introducing the chosen kinematics, we find the following expression for the kinetic energy:

$$T(u_1,u_3,\theta,\beta) = T^r + T^s + T^{rs} \text{ with } \begin{cases} T^r = \displaystyle\int_0^L \frac{1}{2}\left(\rho^s a\left(\dot{u}_1^2 + \dot{u}_3^2\right) + \rho^s\,\overline{z^2}\,\dot{\theta}^2\right) ds_1 \\ T^s = \displaystyle\int_0^L \frac{1}{2}\rho^s\left(\dot{\overline{y^2 + z^2}}\right) ds_1 \\ T^{rs} = \displaystyle\int_0^L \rho^s\left(-\dot{u}_1\,\dot{\overline{(z\sin\theta)}} + \dot{u}_3\,\dot{\overline{(z\cos\theta)}}\right) ds_1 \end{cases} \tag{10}$$

where the notation $\dot{X}$ stands for the time derivative of X.

3 Numerical implementation

For the numerical simulations we used the FE software COMSOL to solve the weak formulation of the elastodynamic problem obtained from our 1D model applying the Hamilton principle. Indeed, COMSOL offers the possibility to introduce directly the weak form of the expressions for the elastic and kinetic energy densities and is able to proceed to an analytical differentiation of these expressions. Only the kinetic energy T has required an explicit calculus of variations because an integration by parts with respect to time was needed to obtain its weak form. A Lagrange multiplier (5th degree of freedom) is used to constrain the relation between the translations u_1 and u_3 and the rotation θ. And a finite element discretisation of the rod line is done before solving this constraint problem for the stationnary points of the Hamiltonian.

4 Numerical results

In the following, three tests are presented to illustrate the model ability to account for complex scenarios of folding, coiling and deployment, in statics and dynamics. The geometrical and material properties used for these tests are given in Tables 1 and 2.

Table 1: Geometrical properties of the tape spring.

Length L	Width a	Thickness h	Initial angle β_0^e
1170 mm	60 mm	0.15 mm	0.6 rad

Table 2: Material properties of the tape spring.

Young's modulus E	Poisson's ratio ν	Density ρ
210 000 MPa	0.3	7800 kg.m^{-3}

For all the following results, the mesh of the rod line was made of 60 Hermite quintic finite elements (1210 degrees of freedom) and the default implicit time-dependent solver of COMSOL (BDF solver) was used with a variable time-step and a numerical damping handled automatically. The three-dimensional deformed shapes presented hereafter are reconstructed using the kinematics exposed at Section 2.1 from the results of $u_1(s_1)$, $u_3(s_1)$, $\theta(s_1)$ and $\beta^e(s_1)$ obtained with the 1D extended rod model. And the color plots, which illustrate the curvature of the cross-section curve, are those of angle β.

4.1 Coiling of a tape spring

This first test illustrates the model simplicity in terms of simulation driving. Indeed, with this model it becomes very intuitive to drive the opening and the rotation of a cross-section. Direct access to the variable β^e in COMSOL allows localized openings as well as various driving scenarios for cross-section rotation through direct application of an appropriate loading relative to this variable. The easiness in driving the cross-section opening and rotation makes it possible to reach many folded configurations.

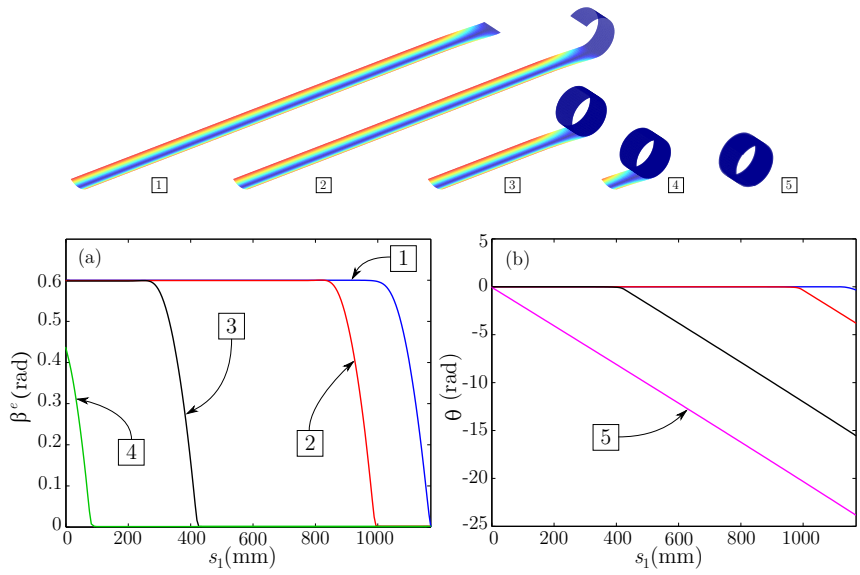

Figure 3: Coiling of a tape spring.

It is thus very simple to simulate the coiling of a tape spring in statics as shown in Figure 3. We only need to flatten and maintain flattened one of the tape spring extremities, before imposing a rotation on the associated cross-section. Figure 3 (b) shows that the spring rolls up with a constant and uniform radius. Curve 4 of Figure 3 (a) shows that when the coiled part arrives near the free extremity, the left end cross-section tends to open. If we carry on the test, immediate slackening of the applied load entails

a rough deployment of the tape spring. It is thus necessary to take into account the inertial effects within the framework of dynamics. Therefore the 3rd test presented in this paper will illustrate the dynamic aspect of the model.

4.2 Compressive buckling of a simply supported tape spring

In this second test, the tape spring is submitted to static compressive buckling with both ends free in rotation. The two translational degrees of freedom are constrained at one end whereas the other end is submitted to an horizontal displacement while the vertical displacement is set to zero. The transverse curvature is constrained at both extremities, thus the tape spring is not free to flatten at the ends. To enable the buckling initiation, it is necessary to impose a pre-existing defect. In our case a vertical force of intensity 10^{-4} N is applied at the center of the spring.

Figure 4 (a) illustrates the model ability to account for the snap-through phenomena that occur for this kind of loading [10]. On Figure 4 (b) we compare the shape of β^e along the tape spring just before the appearance of the snap-through phenomenon for buckling by flexion and by compression. This comparison places emphasis on the difference between those two kind of snap-through phenomena. In the case of compressive buckling, we notice a localization of the cross-section opening at the center of the tape spring whereas the cross-section keeps its initial degree of closure near the extremities.

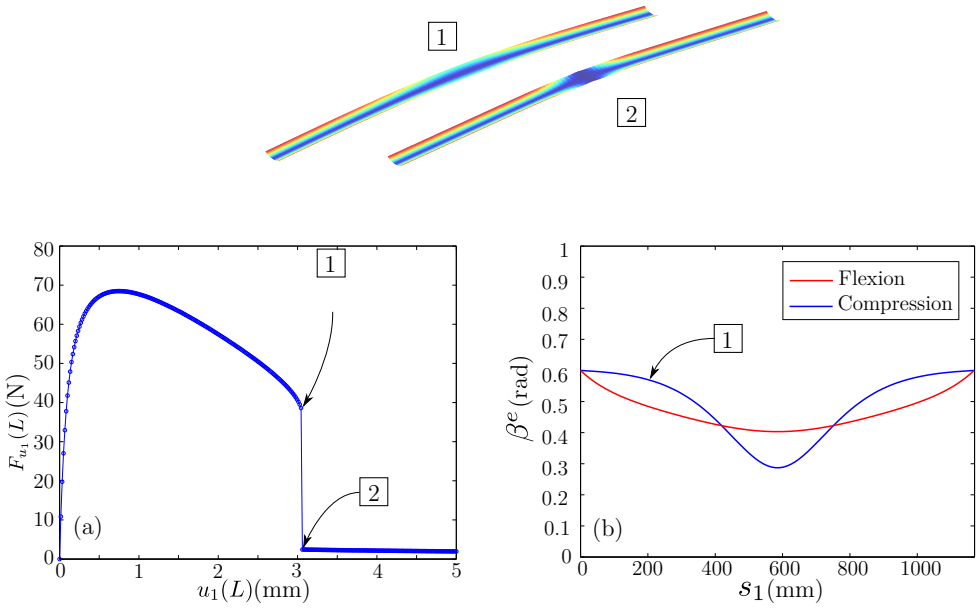

Figure 4: Compressive buckling with both ends free in rotation.

4.3 Deployment of a tape spring with a small folded part

This last example brings to light the effects of inertia and gravity on the deployment of a tape spring in dynamics. The tape, subjected to gravity, is vertical and clamped at the bottom end whereas the other end is folded on a small length (see Figure 5). The folded end is released instantaneously without inital speed. During the first step of deployment, the fold moves down along the tape whereas the free end straigthens up progressively. When the tape goes through the vertical position, the inertial effects cause the formation of a new fold of opposite curvature in the fold area before its complete disappearance. This new fold is also going to move along the tape before it recovers its undeformed shape after a snap-through and a few oscillations around its final position.

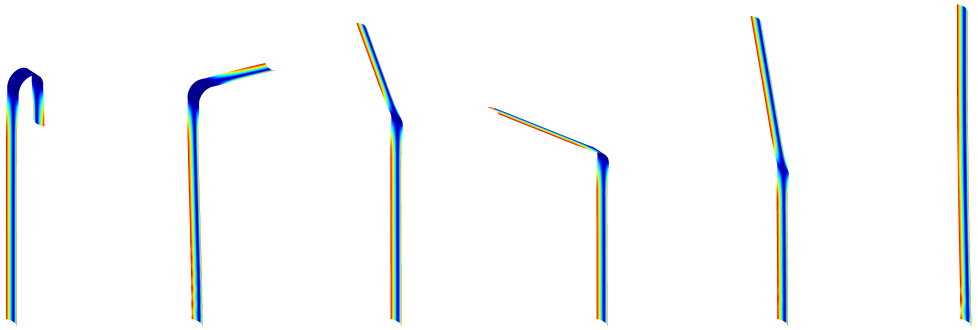

Figure 5: Deployment of a tape spring with a folded part.

We also observe compressive stresses in the vertical arm due to the undulations it undergoes during the second step of deployement. These compressive stresses result in oscillations of the value of β^e near the clamped end (see Figure 6 (a)). It is the tape spring inertia which provokes thoses compressive stresses when the free arm goes through the vertical position and causes as explained before the creation of a new fold. Shortly before going through the vertical position, we also notice a closing of the tape spring cross-sections in the fold area (see Figure 6 (a) curve 6) where the fold of opposite curvature is going to appear.

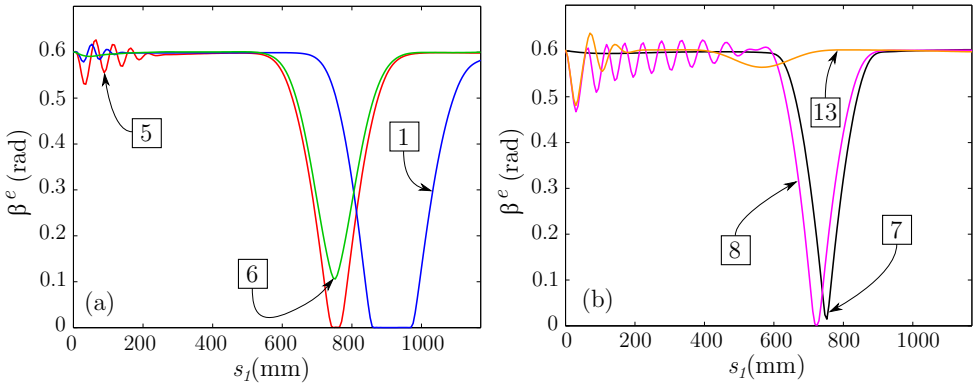

Figure 6: Evolution of β^e during the deployment test.

5 Conclusion

A planar rod model with highly deformable cross-section has been suggested in this paper. This model is suitable for thin-walled and curved cross-sections and accounts for large displacements, large rotations and dynamics. The equations and results presented herein are for the limiting case of in-plane motions but the case of three-dimensional motions including out-of-plane bending and torsion is currently being studied. In both case the approach used is the same. Starting from an energetic approach of a classical nonlinear shell model, an *elastica* kinematics is introduced to account for large changes of the cross-section shape with appropriate shape functions. Moreover beam-like assumptions are done, e.g. by neglecting the transverse membrane stresses with respect to the axial membrane stresses, when expressing the tape spring energy densities. Finally the elastic and kinetic energies are derived, the model is implemented in the FE software COMSOL and the Hamilton principle is used to solve the elastodynamic problem.

The obtained 1D model, which has only four kinematic parameters (for the limiting case of in-plane motions), has been applied to a tape spring and has been used to simulate several sequences of

folding, coiling and deployment. Through these simulations, it has proved its ability to account for several phenomena such as the sudden creation of a fold, the splitting of a fold into two, the inertial or pendulum effects, etc. The generalization of the model to the out-of-plane case, on which we are currently working, should allow to treat more complex folding, coiling and deployment scenarios as well as the planar equal sens folding which requires the consideration of twisting. An extended model may also be used to study the deployment and the stability of more complex structures, made for example of an assembly of tape springs.

References

[1] B. Audoly, Y. Pomeau, *Elasticity and Geometry: From Hair Curls to the Nonlinear Response of Shells*, Oxford University Press, 2010.

[2] E. Euler, *Methodus inveniendi lineas curvas maximi minimive proprietate gaudentes*, 1744.

[3] R. Gonçalves, M. Ritto-Corrêa, D. Camotim, *A large displacement and finite rotation thin-walled beam formulation including cross-section deformation*, Computer Methods in Applied Mechanics and Engineering 199 (23-24), 1627-1643, 2010.

[4] V.G.A. Goss, *The History of the Planar Elastica: Insights into Mechanics and Scientific Method*, Science & Education (18), 1057-1082, 2009.

[5] F. Guinot, *Déploiement régulé de structures spatiales : vers un modèle unidimensionnel de mètre ruban composite*, Doctoral Thesis, Université de Provence, Marseille, 2011.

[6] F. Guinot, S. Bourgeois, B. Cochelin, L. Blanchard, *A planar rod model with flexible thin-walled cross-sections. Application to the folding of tape springs*, International Journal of Solids and Structures, in press, doi:10.1016/j.ijsolstr.2011.09.011.

[7] S. Hoffait, O. Bruls, D. Granville, F. Cugnon, G. Kerschen, *Dynamic analysis of the self-locking phenomenon in tape-spring hinges*, Acta Astronautica 66 (7-8), 1125-1132, 2009.

[8] P. Pimenta, E. Campello, *A fully nonlinear multi-parameter rod model incorporating general cross-sectional in-plane changes and out-of-plane warping*, Latin American Journal of Solids and Structures 1 (1), 119-140, 2003.

[9] M. Santer, S. Pellegrino, *Compliant multistable structural elements*, International Journal of Solids and Structures 45 (24), 6190-6204, 2010.

[10] K. Seffen, S. Pellegrino, *Deployment dynamics of tape springs*, Proceedings of the Royal Society A 455, 1003-1048, 1999.

[11] K. Seffen, Z. You, S. Pellegrino, *Folding and deployment of curved tape springs*, International Journal of Mechanical Sciences 42 (10), 2055-2073, 2000.

[12] N. A. F. Senan, O. M. O'Reilly, T. N. Tresierras, *Modeling the growth and branching of plants: a simple rod based model*, Journal of the Mechanics and Physics of Solids 56 (10), 3021-3036, 2008.

[13] J. Simo, L. Vu-Quoc, *A geometrically-exact rod model incorporating shear and torsion-warping deformation*, International Journal of Solids and Structures 27 (3), 371-393, 1991.

[14] E. Sarostin, G. van der Heijden, *Cascade unlooping of a low-pitch helical spring under tension*, Journal of the Mechanics and Physics of Solids 57 (6), 959-969, 2009.

[15] S. Walker, G. Aglietti, *A study of tape spring fold curvature for space deployable structures*, Proceedings of the Institution of Mechanical Engineers, Part G (Journal of Aerospace Engineering) 221 (G3), 313-325, 2007.